geomatics

MDPI

Article

Reconstruction of Waste Rock Dump Deformation Stages Based on Multi-Temporal UAV Photogrammetry, Terrestrial Laser Scanning, and Mine Surveying

Dmitriy S. Ozhigin, Viktoria V. Kazantseva *, Vera F. Yartseva, Ulpan A. Kubaidullina and Ruslan K. Baigali

Mine Surveying and Geodesy Department, Mining Faculty, Abylkas Saginov Karaganda Technical University, Ave. Nursultan Nazarbayev 56, Karaganda 100027, Kazakhstan
* Correspondence: v.kazantceva@ktu.edu.kz; Tel.: +7-7765080999

Abstract

This study investigates the development of deformation in the southern waste rock dump of the Western Open Pit of the Zhairem Mining and Concentrating Complex through the integrated analysis of multi-temporal geospatial data. The study addresses the need to move beyond the identification of surface changes toward the reconstruction of deformation development and the interpretation of the processes linking changes in dump geometry with the initiation of active displacements. The research is based on the combined use of mine surveying measurements, aerial survey data acquired using UAV, and terrestrial laser scanning. The methodology included the generation and spatial co-registration of multi-temporal digital models, the construction and analysis of cross-sections, the assessment of changes in dump lift geometry and crest positions, and the quantitative evaluation of displacements during the active stage of deformation. The results made it possible to establish the temporal sequence of changes preceding the deformation of the upper dump lift: changes in the geometry of the lower part of the waste rock dump, subsequent restoration of the previously disturbed area through renewed material deposition, and an increase in the height of the upper dump lift. These changes may be considered possible factors contributing to deformation development; however, the available data do not allow their direct causal role to be established. Cross-section No. 2 proved the most informative for reconstructing the deformation sequence, revealing characteristic morphological features, including disturbance of dump lift geometry, elevation loss within the failure zone, and displacements confirmed by terrestrial laser scanning. A comparison of two consecutive terrestrial laser scanning datasets showed pronounced displacements during the first observation interval, whereas during the second interval, the magnitude of the detected changes decreased substantially and was close to the level of metric uncertainty associated with the TLS comparison. The main outcome of this study is the retrospective reconstruction of the successive stages of a deformation event through the integrated analysis of datasets with different spatial and temporal resolutions. The results demonstrate the practical applicability of this approach for analyzing deformation development and supporting the monitoring of waste rock dumps at active mining operations.

Keywords: waste rock dump; deformation process; geotechnical monitoring; photogrammetric processing; terrestrial laser scanning; multi-temporal analysis; unmanned aerial vehicle

Check for updates

Academic Editors: Alessandro Vitale, Guo Chen, Wei Tang, Ling Huang and Amir Allahvirdi-Zadeh

Received: 24 July 2026
Revised: 4 September 2026
Accepted: 18 September 2026
Published: 30 September 2026

Copyright: © 2026 by the authors. Licensee MDPI, Basel, Switzerland. This article is an open access article distributed under the terms and conditions of the Creative Commons Attribution (CC BY) license.

1. Introduction

The current state of mining engineering facilities requires the implementation of systematic geotechnical and mine surveying monitoring to detect deformation processes promptly and prevent hazardous situations [1]. This task is particularly important in open-pit mining operations, where the stability of pit walls, benches, and waste rock dumps directly affects operational safety, the integrity of mining infrastructure, and the continuity of production processes. Effective slope stability monitoring should account not only for the magnitude of displacements, but also for the spatial and temporal evolution of deformation processes [2,3].

Waste rock dumps are among the most challenging objects for geotechnical monitoring, as they are formed under continuous mining activity. During the deposition of overburden material, changes occur in the height and configuration of dump lifts, the rock mass is redistributed, zones with varying degrees of compaction are formed, and previously disturbed or newly deposited areas may become potentially unstable elements of the dump mass [4,5]. The need for regular monitoring and stability control of waste rock dumps has been confirmed by studies demonstrating the effectiveness of photogrammetric data for slope condition assessment [6]. In the investigation of large waste rock masses, the application of realistic three-dimensional models has also been recognized as an effective approach, providing an accurate representation of surface geometry and enabling the identification of potentially unstable zones within the mass [7].

Traditional mine surveying and geodetic observations provide reliable information on the spatial position of characteristic elements of mining facilities. Among the most commonly used instrumental methods are Global Navigation Satellite System (GNSS) measurements and electronic total station surveys. The combination of these technologies remains one of the fundamental approaches to open-pit monitoring, enabling the determination of geodetic control point coordinates and the subsequent total station surveying of characteristic elements of the monitored object [8,9]. The applicability of Real-Time Kinematic (RTK) and Precise Point Positioning (PPP) methods for monitoring deformation, subsidence, and landslide processes in both surface and underground mining conditions has been demonstrated in numerous studies, which have highlighted their high accuracy and reliability in geodynamic monitoring applications [10]. The effectiveness of Continuously Operating Reference Station (CORS) technologies for the real-time monitoring of deformation processes in the waste rock dumps of open pits confirms the importance of high-precision geodetic observations for the stability control of technogenic structures [11].

Despite the high accuracy of instrumental observations, their effectiveness in analyzing complex deformation processes may be limited by the discrete nature of measurements and the local character of the data. GNSS measurements and total station surveys enable recording displacements of individual points, profiles, or control markers; however, they do not provide a spatially continuous representation of the entire surface of the deforming area. In recent years, remote sensing methods for acquiring geospatial data have gained increasing importance, enabling the generation of digital surface models and the multi-temporal comparison of the condition of mining facilities [1,9].

One of the most rapidly developing areas is the use of unmanned aerial vehicles (UAVs) for aerial surveying. UAVs have become a principal tool for monitoring slope stability in open pits due to their operational efficiency, high spatial resolution, and ability to generate digital models [2,3]. UAV-based aerial surveying is regarded as an effective source of spatial data for generating dense point clouds and monitoring deformation processes [12,13]. The effectiveness of integrating aerial survey data with geospatial analysis methods for assessing deformation processes and the stability of open-pit slopes has been confirmed by numerous studies [14,15].

A separate area of research concerns the development of multi-temporal digital models and the analysis of surface changes in technogenic objects. The potential of the dynamic monitoring of mineral deposits through UAV aerial surveys has been demonstrated in studies highlighting the importance of three-dimensional reconstruction for surface change analysis [16]. The applicability of aerial survey data for measuring rock mass displacements has been demonstrated in several studies, confirming the effectiveness of photogrammetric data processing for the quantitative assessment of deformation processes [17]. The effectiveness of UAV-based aerial survey data for monitoring geometric changes in reclaimed embankment structures has also been demonstrated, with the obtained results being applicable to the monitoring of complex-shaped technogenic masses [18].

Multi-temporal aerial survey data primarily reflect changes in object geometry between observation periods, enabling the identification of areas of geometric disturbance, the assessment of changes in crest positions, and the construction of temporal cross-sections. However, when significant intervals exist between surveys, these data do not always provide sufficient information on the short-term dynamics of the active deformation phase. For a reliable interpretation of digital models, comparison with independent geodetic data obtained by instrumental surveying methods is required [9,16].

In this context, terrestrial laser scanning (TLS) should be regarded not as a replacement for GNSS measurements and total station surveys, but as an additional source of dense spatial information on surface geometry. Its main advantage lies in the ability to generate highly detailed point clouds that capture the structural characteristics of local deformation zones. The applicability of three-dimensional TLS for monitoring displacements and landslide processes on open-pit walls has been confirmed by numerous studies [19,20]. The effectiveness of TLS technologies has also been demonstrated in tasks involving detailed mapping, volume estimation, and slope stability assessment under the complex conditions of mining facilities [21,22]. Terrestrial laser scanning is considered a deformation monitoring technology based on the acquisition, comparison, and analysis of point cloud changes, enabling the detection and quantitative assessment of spatio-temporal variations in the geometry of the investigated objects [23,24].

In recent years, increasing attention has been devoted to integrating instrumental geodetic measurements, UAV-based aerial survey data, and laser-scanning technologies. The integration of ground-based and aerial data in open-pit slope modeling improves the completeness of surface representation and compensates for the limitations of individual monitoring methods [25,26]. The combined use of UAV data and terrestrial laser scanning for landslide monitoring enhances the informativeness of deformation analysis, particularly under conditions of limited access to the monitored object [27,28]. The advantages of integrating photogrammetrically processed data and LiDAR datasets are especially evident in slope deformation monitoring, where comparing spatial data with varying levels of detail and completeness is required [29,30].

An analysis of national and international studies shows that a considerable proportion of research is focused either on the generation of digital surface models or on the detection of displacement and changes in slope geometry [31,32]. Less attention has been paid to the reconstruction of deformation process development stages in waste rock dumps using datasets of varying temporal and spatial resolution [33,34]. For such objects, it is important not only to identify the occurrence of surface disturbance, but also to determine which preceding changes in the geometry and internal structure of the dump mass may have contributed to the initiation of deformation processes [35,36]. In this regard, one of the key challenges is to move beyond the detection of spatial changes toward an engineering interpretation of the factors and relationships associated with the development of the deformation process.

Thus, the research gap lies not in the lack of methods for detecting surface changes or measuring displacements, but in the insufficient development of approaches that enable the reconstruction, from multi-temporal data, of the sequence of events preceding the active stage of deformation. The main contribution of this study is the retrospective reconstruction of the stages of an actual deformation event using datasets of varying spatial and temporal resolution, together with an assessment of the possible relationship between preceding changes in waste rock dump geometry and the subsequent development of active displacements.

In the present study, this problem is examined using the southern waste rock dump of the Western Open Pit of the Zhairem Mining and Concentrating Complex as a case study. The research is based on the integrated use of multi-temporal mine surveying measurements, UAV aerial survey data, and terrestrial laser scanning data.

The aim of this study is to reconstruct the stages of waste rock dump deformation development and to assess the possible relationship between preceding changes in its geometry and the subsequent development of active deformation. To achieve this objective, multi-temporal digital models were compared, profile cross-sections were constructed and analyzed, and displacements were quantitatively assessed using terrestrial laser scanning data acquired during the active phase of the deformation process.

2. Materials and Methods

2.1. Characteristics of the Case Study Area

The study area is the southern waste rock dump of the Western Open Pit of the Zhairem Mining and Concentrating Complex, located within the Zhairem deposit (Figure 1). Regionally, the deposit belongs to the Atasu ore district and is one of the major barite-polymetallic deposits of Central Kazakhstan.

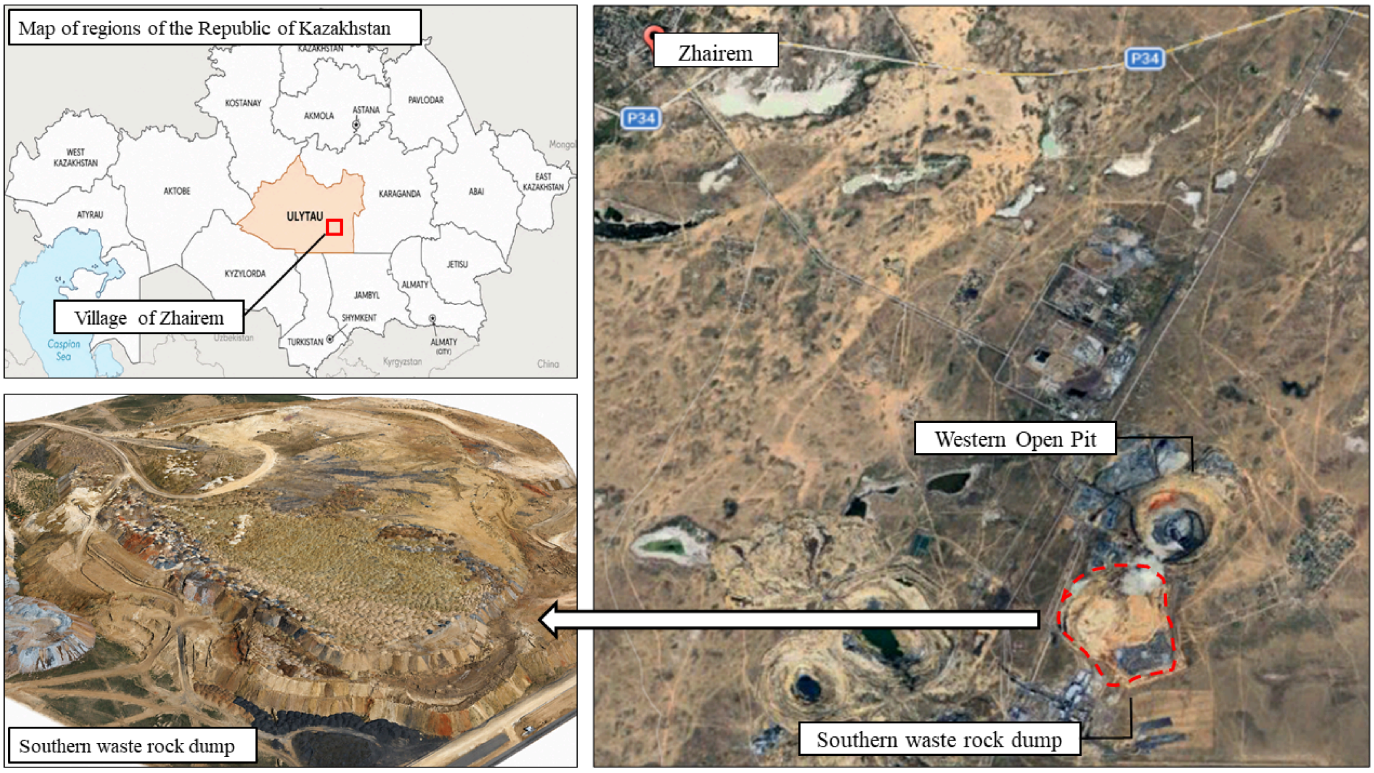


Figure 1. Geographical location of the study area.

The Zhairem deposit is located in the Zhanaarka District of the Ulytau Region, Kazakhstan. The nearest settlement is the village of Zhairem, situated approximately 10 km southeast of the deposit. The nearest industrial centers are the town of Karazhal, 60 km to the southeast; Zhezkazgan, 230 km to the west; and Karaganda, 340 km to the northeast.

The study area is characterized by a predominantly flat terrain with gently undulating low hills. The prevailing surface elevations range from 380 to 425 m above sea level. The climate is sharply continental and semi-arid, with hot summers, cold winters, low precipitation, and a pronounced moisture deficit. The drainage network is poorly developed; the nearest permanent watercourse is the Sarysu River, located approximately 20–25 km north of the deposit.

The southern waste rock dump is one component of the Western Open Pit's mining infrastructure, formed by the deposition of overburden material. The dump is considered an independent technogenic mass, and its spatial position and surface geometry are analyzed. The selection of the southern waste rock dump as the study object is justified by its representativeness as a technogenic formation of the Western Open Pit and by its suitability for investigating changes in dump geometry under active mining conditions.

The study is based on multi-temporal geospatial datasets characterizing the condition of the southern waste rock dump of the Western Open Pit at different observation periods. The dataset includes the results of mine surveying measurements, aerial surveys, and terrestrial laser scanning acquired between 2018 and 2025. The combined use of these data sources enabled an analysis of changes in dump geometry over both long-term observation periods and short-term intervals associated with active displacement processes. The main datasets used in the study and their respective roles are summarized in Table 1.

Table 1. Sources of the geospatial data used in the study.

Observation Period	Data Type	Equipment	Primary Output
2018	Mine surveying measurements	GNSS, Trimble R10 (Trimble Inc., Westminster, CO, USA)	Profile data on crest positions and slope geometry
2019	UAV aerial survey	UAV, VolJet X8GEO (VolJet, Moscow, Russia)	Orthomosaic, DSM
2021	Mine surveying measurements	GNSS, Trimble R10 Trimble Inc., Westminster, CO, USA	Profile data on crest positions and slope geometry
2022	Mine surveying measurements	GNSS, Trimble R10 (Trimble Inc., Westminster, CO, USA)	Profile data on crest positions and slope geometry
2022	UAV aerial survey	UAV, DJI Mavic 2 Pro PPK (SZ DJI Technology Co., Ltd., Shenzhen, China)	Orthomosaic, DSM
7–9 March 2022	Terrestrial laser scanning	HDS 8800 laser scanner (Leica Geosystems AG, Heerbrugg, Switzerland)	Point cloud, geostructural model
2024	UAV aerial survey	UAV, DJI Matrice 300 RTK (SZ DJI Technology Co., Ltd., Shenzhen, China)	Orthomosaic, DSM
2025	UAV aerial survey	UAV, DJI Mavic 3 Enterprise RTK (SZ DJI Technology Co., Ltd., Shenzhen, China)	Orthomosaic, DSM

Aerial survey data were used to generate multi-temporal digital surface models and orthomosaics required for the spatial comparison of dump conditions at different

observation stages. Mine surveying measurements were employed to compare temporal cross-sections and to analyze changes in dump geometry within characteristic profiles.

Terrestrial laser scanning data were used to obtain highly detailed spatial information on the deformation zone of the upper dump lift and to quantitatively assess displacements over short observation intervals. Thus, the integrated dataset provided a basis for the comprehensive analysis of the deformation process, including the identification of areas affected by surface geometry changes, the construction of multi-temporal profiles, and the assessment of displacement dynamics during the active phase of deformation.

2.2. UAV-Based Aerial Photography and Photogrammetric Processing

Aerial surveys were conducted using various types of UAV, selected based on the survey area, object configuration, and data-acquisition requirements. Over the course of the study, the VolJet X8GEO, DJI Mavic 2 Pro PPK, DJI Matrice 300 RTK, and DJI Mavic 3 Enterprise RTK UAV platforms were employed.

Aerial surveys were conducted according to pre-planned flight missions designed to achieve the required forward and side image overlap. Flight parameters, including survey altitude, image overlap, and spatial resolution, were selected based on the size of the study area, the geometry of the waste rock dump, and the required level of detail for the resulting digital models. The main aerial survey parameters for the different UAV platforms used in this study are presented in Table 2.

Table 2. UAV aerial survey parameters by observation series.

UAV	Camera	Survey Year	Positioning Method	Flight Altitude, m	Forward Overlap, %	Side Overlap, %	Ground Sampling Distance, cm/Pixel	Focal Length, mm
VolJet X8GEO	Sony Alpha 7 (Sony Corporation, Tokyo, Japan)	2019	PPK	150	80	70	2.4	28
DJI Mavic 2 Pro PPK	Hasselblad L1D-20c, 1″ CMOS, 20 MP (Hasselblad, Gothenburg, Sweden)	2022	PPK	150	85	70	3.5	10
DJI Matrice 300 RTK	DJI Zenmuse P1, full-frame CMOS, 45 MP, 35 mm lens (SZ DJI Technology Co., Ltd., Shenzhen, China)	2024	RTK	550	70	60	8.0	35
DJI Mavic 3 Enterprise RTK	4/3 CMOS wide camera, 20 MP (SZ DJI Technology Co., Ltd., Shenzhen, China)	2025	RTK	186	80	70	5.0	12

For georeferencing the aerial imagery, the coordinates of the image projection centers determined by the onboard GNSS receivers of the UAVs in PPK or RTK mode, depending on the observation series, were used. A single permanent GNSS base station located within the Zhairem Mining and Concentrating Complex was used for all aerial surveys. The study area was located approximately 5–7 km from the base station. The station continuously recorded raw satellite observations for subsequent PPK processing and transmitted differential corrections via GSM during surveys conducted in RTK mode.

The accuracy values of up to 10 mm horizontally and 30 mm vertically represent the specified accuracy level of the equipment used and are not considered the actual accuracy achieved by the final photogrammetric models. We assessed the actual accuracy of the generated models separately using geodetic control points and present it in Table 3.

Table 3. Photogrammetric processing results and model accuracy.

Survey Year	UAV Platform	Number of Images	Positioning Method	Ground Sampling Distance (GSD), cm/Pixel	Mean Camera Position Adjustment, mm	RMSE at Check Points, mm	RMSE at GCPs, mm
2019	VolJet X8GEO	1043	PPK	2.4	97	18	11
2022	DJI Mavic 2 Pro PPK	198 (western sector)	PPK	3.5	94	35	13
2024	DJI Matrice 300 RTK	952	RTK	8.0	155	56	21
2025	DJI Mavic 3 Enterprise RTK	670	RTK	5.0	20	16	9

Depending on the UAV platform, the following positioning methods were employed:

- Post-Processed Kinematic (PPK)—post-processing of kinematic GNSS observations after the flight to improve positioning accuracy. This method was used, for example, with the DJI Mavic 2 Pro PPK.
- Real-Time Kinematic (RTK)—real-time positioning based on communication with a reference station, providing high-accuracy image georeferencing during data acquisition. This method was employed with the DJI Mavic 3 Enterprise RTK and DJI Matrice 300 RTK.

For the processing of survey datasets acquired in PPK mode, raw satellite observations from the permanent base station were used. Post-processing of the kinematic GNSS data was performed using Emlid Studio version 1.9. For surveys conducted in RTK mode, corrections from the same base station were transmitted to the onboard GNSS receiver of the UAV via GSM in real-time.

A network of 10 marked geodetic points, whose coordinates were determined using GNSS measurements, was used for the generation and independent accuracy assessment of the photogrammetric models. Four points (M1, M2, M5, and M6) were used as ground control points (GCPs) and included in the photogrammetric adjustment. The remaining six points (M3, M4, M7, M8, M9, and M10) were excluded from the adjustment and used as independent check points to assess the spatial accuracy of the resulting models. The spatial distribution of the ground control points and check points is shown in Figure 2. The RMSE values at the ground control points and check points for each observation series are presented in Table 3.

The aerial surveys provided the source data required for subsequent photogrammetric processing and the development of the digital foundation for this study.

Photogrammetric processing of the aerial survey data was performed using Agisoft Metashape version 1.8. A consistent processing workflow was applied to all observation series, including image alignment, refinement of camera parameters, dense point cloud generation and filtering, digital surface model generation, and orthomosaic generation (Figure 3). Image alignment was performed at Medium accuracy, with the Key point limit set to 40,000 and the Tie point limit to 4000. During photogrammetric adjustment, automatic camera calibration was performed, followed by optimization of the camera parameters. The dense point cloud was generated using the Quality setting of High and the Depth filtering mode set to Aggressive. After point cloud generation, additional filtering based on confidence values was performed, excluding points with confidence values from 0 to 3 from further processing.



Figure 2. Distribution of ground control points (GCPs) and independent check points used for photogrammetric model generation and accuracy assessment.

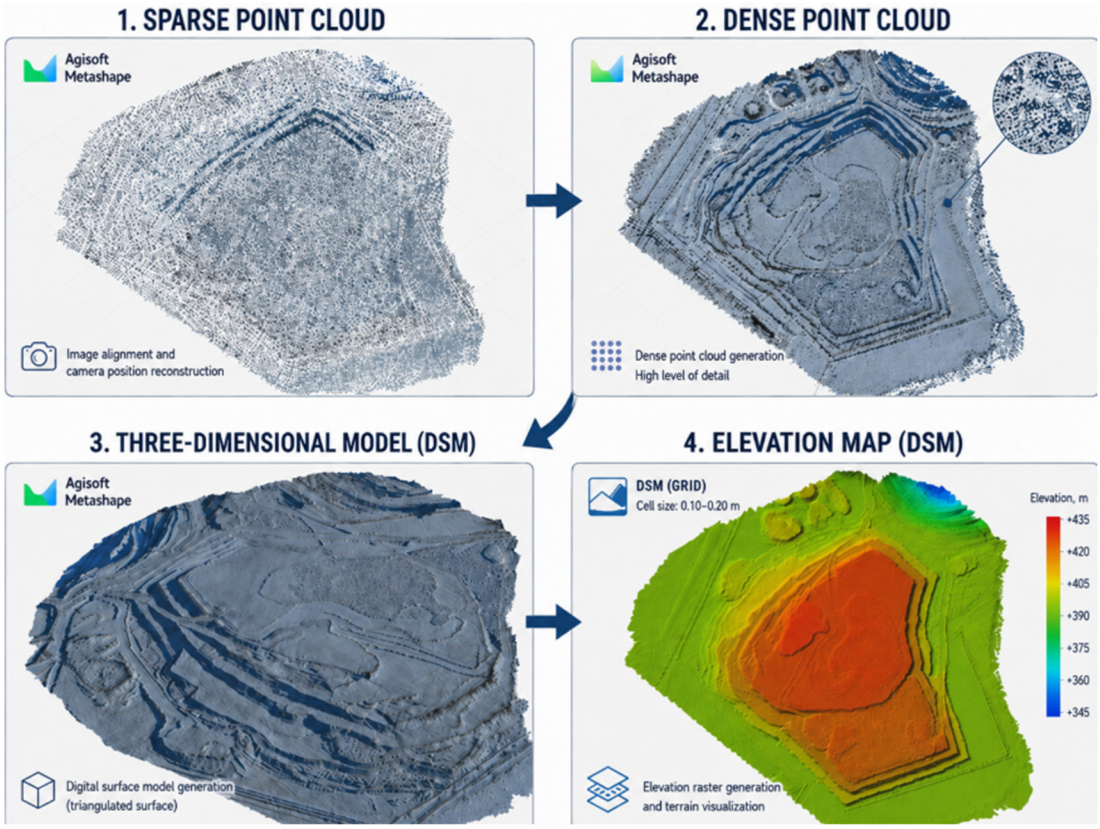


Figure 3. Photogrammetric workflow for geospatial data processing in Agisoft Metashape.

During photogrammetric processing, the coordinates of the camera projection centers recorded by the UAV platforms' onboard GNSS receivers were used. Depending on the UAV platform, image georeferencing was based on either PPK or RTK positioning, providing the accuracy required for exterior orientation and subsequent three-dimensional reconstruction. The resulting digital models were transformed into a common coordinate system, providing a consistent spatial reference for their subsequent multi-temporal comparison.

Digital models of the southern waste rock dump of the Western Open Pit were generated from the aerial survey data acquired in 2019, 2022, 2024, and 2025. The consistent processing workflow and the use of a standardized set of output products provided a comparable multi-temporal digital dataset for the subsequent analysis of changes in dump geometry.

The quality of the photogrammetric processing was assessed based on the spatial resolution of the resulting models, the magnitude of camera position adjustment during photogrammetric adjustment, and the RMSE values at the ground control points and independent check points. The Mean camera position adjustment represents the average change in the estimated position of the camera projection centers after photogrammetric adjustment relative to their initial coordinates obtained using PPK or RTK positioning. This parameter characterizes the degree of adjustment of the exterior orientation parameters during processing, whereas the spatial accuracy of the final photogrammetric models was assessed using the RMSE values obtained at the independent check points. The main processing results and model accuracy characteristics are presented in Table 3.

DSMs and orthomosaics generated through photogrammetric processing were integrated into a common geospatial environment for subsequent multi-temporal analysis.

2.3. Creation and Co-Registration of Multi-Temporal Digital Models

The datasets were integrated in Leapfrog Geo, where the point clouds, digital surface models (DSMs), and other spatial data were imported. This provided centralized data storage, visualization, and spatial co-registration of the models generated from datasets acquired during different observation periods (Figure 4).

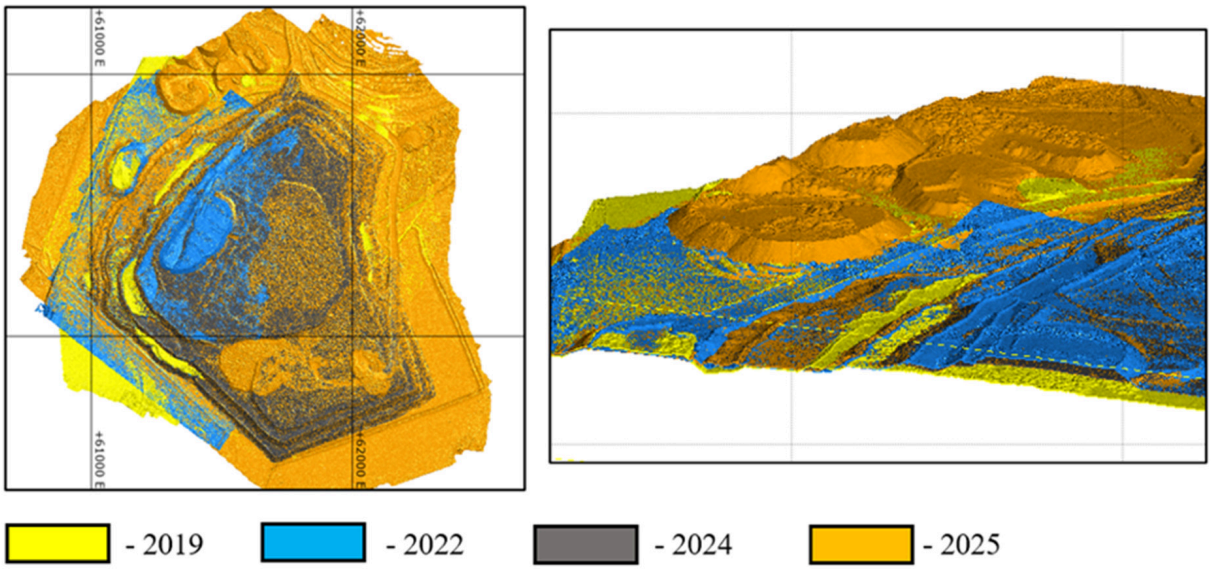


Figure 4. Spatial co-registration of digital models of the southern waste rock dump. Color coding is used to visually distinguish the models by observation series and to identify areas of changes in waste rock dump geometry.

At the first stage, all digital models generated through photogrammetric processing were transformed into a common coordinate system and integrated into a shared geospatial environment. Transforming the datasets into a common coordinate system provided a consistent spatial reference for multi-temporal comparison; however, it did not eliminate residual errors associated with georeferencing and digital model generation. The relative spatial consistency of the models from different observation periods was controlled using the same network of geodetic points employed across all observation series. In particular,

six independent check points that were not included in the photogrammetric adjustment were used to independently assess the accuracy of each model. No additional surface-based forced co-registration of the multi-temporal models was performed, because the waste rock dump surface itself was the object of analysis and could change between observation periods. The residual uncertainty in the relative positioning of the models was accounted for using the RMSE values at the independent check points and was subsequently used to determine the limit of detection (LoD) for surface changes.

The accuracy of the source data was taken into account when assessing the reliability of the multi-temporal comparison. The 2018 mine surveying measurements were performed using a Trimble R10 GNSS receiver in RTK mode; the manufacturer-specified root-mean-square accuracy for this mode is ±8 mm + 1 ppm horizontally and ±15 mm + 1 ppm vertically. For the 2022 photogrammetric model, the RMSE at the independent check points was 35 mm, whereas the RMSE at the ground control points included in the adjustment was 13 mm. The more conservative RMSE value obtained at the independent check points was used to assess the reliability of the multi-temporal comparison. Thus, the errors associated with both methods are on the order of centimeters, whereas the elevation decrease identified within the deformation zone along Cross-section No. 2 was 12.07 m. The detected change exceeded the accuracy level of the source data by more than two orders of magnitude, confirming its reliability. At the same time, residual errors associated with georeferencing and digital model generation may substantially affect changes at the centimeter scale; therefore, differences comparable to the accuracy of the source data were not used to interpret the deformation process.

In addition to accuracy, differences in UAV aerial survey parameters were considered when assessing the comparability of the multi-temporal models. The ground sampling distance (GSD) values of the individual survey datasets ranged from 2.4 to 8.0 cm/pixel, while the corresponding RMSE values are presented in Table 3. An increase in GSD reduces surface detail and may result in the smoothing of local morphological features. Therefore, the multi-temporal photogrammetric models in this study were used primarily to analyze large-scale changes in waste rock dump geometry. The detected meter-scale changes substantially exceeded the RMSE range of the models used (16–56 mm), whereas changes comparable to the accuracy level of the source models were not used to interpret the deformation process.

To quantitatively distinguish reliable surface changes from changes within the accuracy limits of the models, the LoD was additionally determined. The RMSE values at the independent check points presented in Table 3 were used to estimate the uncertainty for each observation epoch. For consecutive pairs of models, the calculated LoD at the 95% confidence level was approximately 0.08 m for 2019–2022, 0.13 m for 2022–2024, and 0.11 m for 2024–2025. Changes that did not exceed the corresponding threshold were not considered reliable changes in surface geometry.

Color-based comparison of the multi-temporal digital models was used primarily to spatially identify areas exhibiting the most pronounced changes in surface geometry and was not considered an independent quantitative criterion of deformation. Quantitative assessment of the changes was performed using multi-temporal cross-sections, enabling the combined analysis of photogrammetric models and mine surveying measurements represented as profile data. The reliability of the detected changes was assessed by considering the accuracy at the independent check points and the calculated LoD values. The profile-based approach was selected because of the heterogeneity of the source time series, which included mine surveying measurements, photogrammetric models, and terrestrial laser scanning data with different spatial and temporal resolutions.

The second stage involved loading and jointly visualizing multi-temporal digital models. To facilitate the interpretation of temporal differences, the models were displayed using color coding by survey year. This approach enabled the identification of areas exhibiting spatial discrepancies between successive surface models, the detection of changes in the configuration of crests and dump lifts, and the assessment of rock mass redistribution within the study waste rock dump.

At the final stage, the co-registered models were used as a unified digital dataset for subsequent analysis. Their comparison enabled the identification of the areas exhibiting the most pronounced changes in surface geometry. These areas were subsequently selected as priority locations for constructing cross-sections and performing a detailed analysis of the deformation process.

The integration of the multi-temporal digital models provided a comprehensive spatio-temporal representation of the geometric evolution of the southern waste rock dump. This made it possible to identify areas exhibiting the most pronounced surface changes, which were subsequently selected for detailed investigation.

2.4. Terrestrial Laser Scanning and Data Processing

To investigate the deformation zone of the upper dump lift in greater detail, terrestrial laser scanning was conducted in March 2022 using a Leica HDS 8800 laser scanner. This survey method was selected to obtain highly detailed spatial information on surface geometry over short observation intervals, which is particularly important for monitoring active deformation processes. Unlike multi-temporal aerial surveys, which are primarily used to analyze changes in dump geometry over different observation periods, terrestrial laser scanning provides a detailed representation of the deformation zone during the active stage of deformation.

Each terrestrial laser scanning survey was conducted from three scanner positions arranged to provide overlap between the point clouds and the most complete possible coverage of the investigated deformation zone. At each position, the scanner was set up over a geodetic point with known coordinates and oriented toward another point with a known horizontal and vertical position, allowing each scan to be directly referenced to the adopted coordinate system. Artificial targets or stable surface features were not used for subsequent forced co-registration of the point clouds. Scanning was performed at density setting 8 with an angular step of approximately 0.025°. At a representative distance of approximately 100 m from the investigated surface, the linear spacing between adjacent measurements was approximately 44 mm. The present study used data acquired during two consecutive observation intervals: from 11:00 on 7 March 2022 to 17:00 on 8 March 2022, and from 17:00 on 8 March 2022 to 11:00 on 9 March 2022. The layout of the scanner positions and scanning directions within the southern waste rock dump is shown in Figure 5.

Terrestrial laser scanning data were processed using Maptek I-Site Studio version 2025.3. The processing workflow included the import, registration, and co-registration of point clouds acquired during individual observation periods, noise filtering, generation of a three-dimensional spatial model of the study area, and preparation of the data for subsequent analysis.

The quality of the relative alignment of the scans within each survey series was assessed using overlapping areas of the point clouds. The root-mean-square (RMS) discrepancy between corresponding overlapping areas did not exceed 12–15 mm. After verification of the spatial alignment quality, the three scans from each survey series were merged into a single point cloud. During filtering, isolated outliers and points located outside the investigated surface were removed. Consecutive survey series were compared using Maptek

I-Site Studio, and the magnitudes of change were determined from the multi-temporal surface positions along the analyzed profiles.



Figure 5. Layout of terrestrial laser scanning of the southern waste rock dump, showing scanner stations and scanning directions.

To assess the metric significance of changes between consecutive TLS survey series, a change detection threshold was additionally determined. The maximum RMS value for point cloud alignment, equal to 15 mm, was adopted as an estimate of the registration uncertainty for each survey series. Accounting for uncertainty propagation when comparing two consecutive survey series, the calculated change detection threshold at the 95% confidence level was approximately 42 mm. This threshold characterizes the uncertainty component associated with point cloud alignment; the effects of surface roughness, scanning geometry, and local variations in point density were not assessed separately. Therefore, changes not exceeding 42 mm were not interpreted in this study as metrically reliable changes in surface position.

When comparing consecutive TLS survey series, the same material points within the waste rock mass were not tracked. The measured values represent the distances between corresponding surface positions along the analyzed profiles and are therefore referred to hereafter as surface/profile offsets rather than direct displacements of identical material points within the rock mass.

3. Results

The comparison of the multi-temporal digital models of the southern waste rock dump of the Western Open Pit, generated from the aerial survey data, revealed areas

affected by changes in surface geometry. The most significant changes were identified in the southwestern part of the dump, where deformation involved a group of dump lifts and was accompanied by changes in crest positions, redistribution of the rock mass, and loss of surface integrity.

The identified spatial differences made it possible to delineate the zone where surface geometry changes were most pronounced and therefore required detailed analysis using cross-sections. Unlike areas where surface changes were primarily associated with routine waste rock deposition, this zone was selected for further investigation because of the nature and magnitude of the observed geometric changes.

To investigate the areas identified through comparison of the multi-temporal models in greater detail, a series of cross-sections was constructed in Agisoft Metashape. Their locations were selected based on the configuration of the detected geometric changes, the surface morphology of the waste rock dump, and the positions of the dump crests. The spatial arrangement of the cross-sections on the southern waste rock dump is shown in Figure 6. A total of seven cross-sections were constructed across the study area, covering different parts of the waste rock dump. The cross-sections located in the southwestern part of the dump provided the most informative representation of the deformation process, as the multi-temporal comparison revealed the most significant changes in surface geometry within this area.

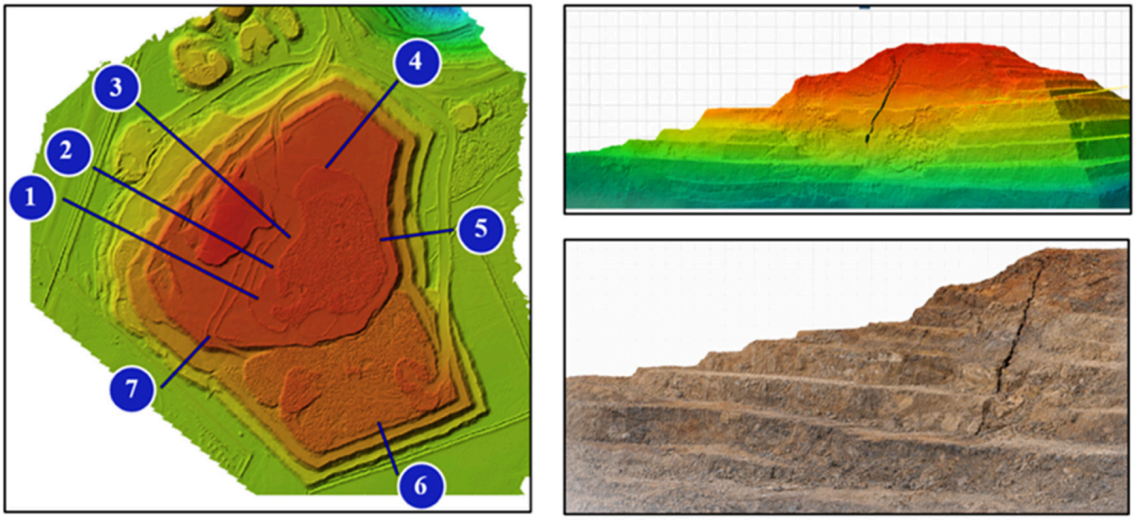


Figure 6. Spatial arrangement and visual representation of cross-sections on the southern waste rock dump of the Western Open Pit.

Of the seven cross-sections constructed, Cross-section No. 2 was selected for detailed multi-temporal analysis based on several criteria. It crosses the southwestern part of the waste rock dump, where the co-registration of the digital models revealed the most pronounced changes in surface geometry. At the same time, this cross-section captures changes in both the lower and upper dump lifts, including changes in crest positions and the development of a tension crack. In addition, a sequential series of mine surveying and photogrammetric data is available along this cross-section, enabling changes in waste rock dump geometry to be traced over the 2018–2022 period, and its location coincides with the area for which terrestrial laser scanning data were acquired in March 2022. Thus, Cross-section No. 2 was selected not only because of the pronounced deformation, but also because it enabled data obtained using different observation methods to be compared within a single profile over successive stages of the deformation process.

The multi-temporal comparison of Cross-section No. 2, constructed from mine surveying measurements and aerial survey data, showed that the geometry of the waste rock dump evolved progressively as a result of rock mass redistribution within the lower and upper dump lifts. The comparison of the 2018 and 2019 profiles revealed the initial geometric changes in the lower dump lift at the +404 m bench level, caused by excavation of part of the rock mass. As a result, the profile elevation decreased to the +394 m bench level, while the front of the dump advanced by 63.19 m, indicating a substantial change in the geometry of the lower part of the waste rock dump.

In 2021, the previously excavated area of the lower dump lift was restored through renewed deposition of waste rock material. The design scheme for waste rock dump construction involved the sequential deposition of material followed by consolidation at each level and did not provide for the subsequent excavation and restoration of an already formed waste rock mass. Thus, the restored area differed from the main part of the lower dump lift in terms of its formation conditions and sequence.

Thus, by the beginning of 2022, the study area was characterized by altered geometry of the lower dump lift and the presence of a part of the waste rock mass restored through renewed material deposition, whose formation conditions differed from the design sequence of material deposition and consolidation.

An additional change in waste rock dump geometry in early 2022 was the formation of the upper dump lift. According to the available data, by February 2022, its height had increased by approximately 17 m, resulting in increased loading on the underlying part of the waste rock mass. As early as March 2022, failure of the bench at the +444 m bench level was identified in the upper dump lift through comparisons of mine survey measurements and aerial survey data.

The comparison of the mine surveying profile and the 2022 aerial survey data revealed a 12.07 m decrease in elevation within the deformation zone relative to the upper dump lift profile recorded in February 2022 (Figure 7). The established sequence shows that the deformation of the upper dump lift in March 2022 was preceded by changes in the geometry of the lower dump lift, its subsequent restoration through renewed material deposition, and an increase in the height of the upper dump lift. The obtained data allow the deviation from the design sequence of lower dump lift formation and the subsequent surcharge to be considered as possible factors contributing to deformation development; however, in the absence of direct geotechnical measurements, their influence on stability was not quantitatively assessed.

Thus, the analysis of the multi-temporal profiles along Cross-section No. 2 made it possible to reconstruct the sequence of geometric changes within the waste rock dump and identify the principal morphological features of deformation affecting the upper dump lift. However, confirming the ongoing activity of the deformation process and quantifying displacements over a short observation interval required the use of terrestrial laser scanning data. The incorporation of these data extended the analysis from the assessment of geometric changes between successive observation periods to the investigation of the deformation process during its active stage.

While the multi-temporal profiles derived from mine surveying measurements and aerial survey data enabled the reconstruction of the geometric evolution of the waste rock dump, terrestrial laser scanning provided quantitative information on displacements during the active phase of the deformation process.

Analysis of cross-sections derived from terrestrial laser scanning data acquired between 11:00 on 7 March 2022 and 17:00 on 8 March 2022 indicated that the deformation zone remained highly active.

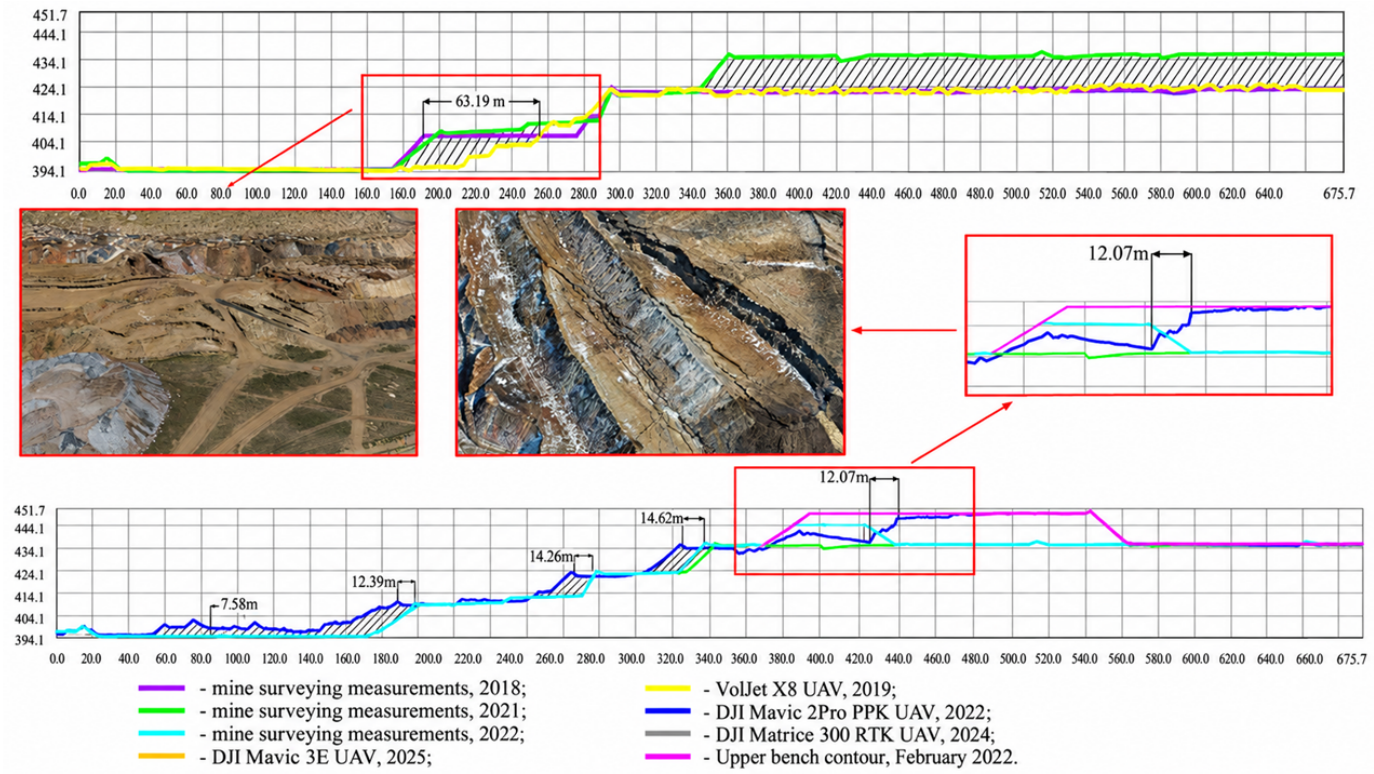


Figure 7. Cross-section No. 2 of the southern waste rock dump of the Western Open Pit.

Along Cross-section No. 2, horizontal surface/profile offsets were recorded at the +431, +422, +413, and +407 m levels during the first observation interval; their quantitative values are presented in Table 4. Selected representative areas at the +431, +422, and +407 m levels are shown in Figure 8. In addition, a vertical displacement of +105 mm was measured at the +407 m bench level, indicating that the deformation process involved not only horizontal redistribution of the rock mass, but also vertical modification of the geometry of the upper dump lift (Table 4).

Table 4. TLS-derived surface-profile offsets in the deformation zone of Cross-section No. 2.

Observation Interval	Bench Level	Horizontal Profile Offset, mm	Vertical Profile Offset, mm	Displacement Rate, mm/day
11:00 7 March 2022–17:00 8 March 2022	+431	242	–	194
	+422	183	–	146
	+413	201	–	161
	+407	226	+105	199
17:00 8 March 2022–11:00 9 March 2022	+414	32	–	43
	+405	24	–	32

The results of the second terrestrial laser scanning survey, conducted during the subsequent observation interval from 17:00 on 8 March to 11:00 on 9 March 2022, showed substantially smaller changes in surface position compared with the first interval. Along Cross-section No. 2, horizontal surface/profile offsets of 32 and 24 mm were recorded at the +414 and +405 m levels, respectively. Both values were below the LoD_{95} threshold of approximately 42 mm calculated for the TLS comparison and therefore cannot be regarded as metrically reliable evidence of continued movement of the waste rock mass. They indicate only that the surface changes during the second observation interval were within the uncertainty level of the applied comparison method.

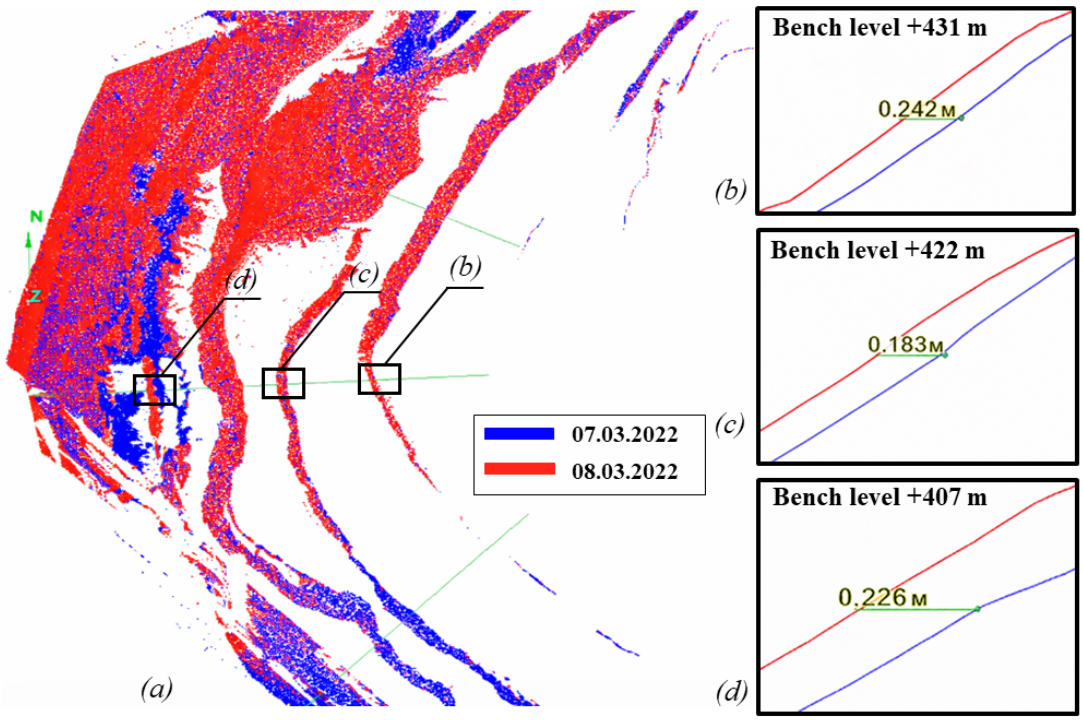


Figure 8. Results of terrestrial laser scanning of the deformation zone: (**a**) overall co-registration of point clouds; (**b**) detailed view of surface-profile offset at Level +431 m; (**c**) detailed view of surface-profile offset at Level +422 m; (**d**) detailed view of surface-profile offset at Level +407 m. The blue point cloud corresponds to the earlier TLS survey series acquired on 7 March 2022, whereas the red point cloud corresponds to the subsequent survey series acquired on 8 March 2022. The orientation indicator shows north. Surface-profile offsets were determined in Maptek I-Site Studio as the distances between corresponding surface positions derived from two consecutive scans. The complete quantitative results for all analyzed levels are presented in Table 4.

The comparison of the two consecutive terrestrial laser scanning surveys indicates that the deformation process developed in a non-uniform, stage-wise manner. During the first observation interval, changes in surface/profile position were more pronounced and included both horizontal and vertical components. During the second interval, the magnitude of the detected changes decreased substantially and fell below the calculated LoD95 threshold. Therefore, the available data do not allow continued deformation activity during this interval to be reliably confirmed. Thus, terrestrial laser scanning enabled capture of the active stage of the deformation process and quantitatively characterizing its short-term evolution.

The displacement rate was calculated as the resultant change in surface position divided by the duration of the corresponding observation interval. Where only the horizontal component was recorded, the resultant value corresponded to the horizontal surface/profile offset. At the +407 m level, the resultant value was calculated using the horizontal component of 226 mm and the vertical component of +105 mm. The rates presented in the table were rounded to the nearest whole millimeter per day, taking into account the metric accuracy of the TLS comparison. However, the changes of 24 and 32 mm obtained during the second observation interval were below the established change detection threshold of 42 mm; therefore, the corresponding rates were not interpreted as metrically reliable rates of deformation movement.

Subsequent aerial surveys conducted in 2024 and 2025 made it possible to assess the condition of the deformation zone following the events of March 2022. By that time, the upper dump lift formed in early 2022, which had imposed additional loading on

the underlying part of the rock mass, had been removed. Comparison of the 2024 and 2025 datasets revealed no further development of large-scale geometric changes within the study area comparable to the deformation recorded in March 2022. This indicates that large-scale changes in surface geometry had stabilized by the time of the subsequent observations. However, the absence of continuous instrumental observations between March 2022 and the 2024 survey did not allow for the exact timing of stabilization of the deformation process to be determined, or any short-term intermediate phases of renewed deformation activity to be identified.

Overall, the analysis made it possible to reconstruct the sequence of processes linking changes in the geometry of the lower part of the waste rock dump, the subsequent surcharge of the upper dump lift, and the development of deformation within this zone. The multi-temporal aerial survey data and mine surveying measurements enabled the reconstruction of the overall sequence of morphological changes within the waste rock dump, whereas terrestrial laser scanning provided a quantitative characterization of displacements during the active stage of deformation. Collectively, these results indicate that deformation of the investigated area evolved progressively and exhibited pronounced temporal variability. Thus, the analysis made it possible to trace the evolution of the study area from the preceding geometric changes and active deformation in March 2022 to the stabilized condition recorded by the subsequent aerial surveys conducted in 2024 and 2025.

4. Discussion

4.1. Reconstructing the Deformation Development Mechanism from Multi-Temporal Data

The results demonstrate that integrating multi-temporal aerial survey data with high-frequency terrestrial laser scanning enables the analysis of deformation processes across different temporal scales. The aerial survey data enabled a reconstruction of the long-term geometric evolution of the southern waste rock dump of the Western Open Pit, identification of the area exhibiting the most pronounced changes, and establishment of the sequence of morphological transformations of the waste rock dump. In turn, the terrestrial laser scanning data provided a quantitative assessment of displacements over short observation intervals, thereby refining the characterization of the active stage of deformation. The combined application of these methods enabled the transition from general spatio-temporal characterization of the deformation process to a detailed assessment of its kinematic behavior.

A key outcome of this study is the reconstruction of the sequence of geometric changes within Cross-section No. 2. The analysis of the multi-temporal profiles showed that the first stage was characterized by geometric disturbance of the lower dump lift caused by excavation of part of the rock mass. At the next stage, the previously excavated area of the lower dump lift was restored through the renewed deposition of waste rock material. This sequence differed from the design scheme for waste rock dump construction, which involved the sequential deposition and consolidation of material at each level without subsequent excavation and restoration of an already formed waste rock mass. In early 2022, the increase in the height of the upper dump lift imposed additional loading on the restored part of the lower dump lift, after which deformation was recorded in March 2022. This sequence allows the deviation from the design sequence of lower dump lift formation and the subsequent surcharge to be considered as possible factors contributing to the development of the deformation process. However, their influence on stability was not quantitatively assessed because direct data on the density, degree of consolidation, and strength characteristics of the restored material were unavailable.

The positive vertical profile-offset component of +105 mm recorded by terrestrial laser scanning at the +407 m bench level may be associated with local uplift or bulging of the

rock mass in the lower part of the deformation zone resulting from material redistribution during displacement of the overlying part of the waste rock dump. The obtained data indicate that the deformation process involved not only horizontal surface changes, but also local changes in the vertical geometry of the rock mass. However, the available data characterize surface changes only and do not allow the failure mechanism or the position of the slip surface to be determined unambiguously. A quantitative stability assessment, including calculation of the factor of safety, would require additional data on the physical and mechanical properties of the rock material and the internal structure of the waste rock dump, which were not determined within the scope of this study.

4.2. Role of Terrestrial Laser Scanning and Practical Value of the Integrated Approach

TLS results confirmed that the deformation identified from the aerial survey data and mine surveying measurements was not a static change in dump geometry but an evolving process. The surface-profile offsets recorded along Cross-section No. 2, which varied in magnitude between consecutive observation intervals, indicate that the deformation process evolved non-uniformly over time. The larger horizontal and vertical surface-profile offsets recorded during the first observation interval, followed by a substantial decrease in the magnitude of changes during the second interval, indicate a reduction in the intensity of the deformation process. During the first interval, the magnitude of the detected changes substantially exceeded the established change detection threshold of 42 mm, confirming pronounced deformation activity. During the second interval, the recorded values of 24–32 mm were below this threshold; therefore, the available data did not allow continued movement to be confirmed with metric reliability or the intensity of the deformation process during this period to be quantitatively characterized.

Thus, terrestrial laser scanning not only confirmed the presence of deformation, but also quantitatively characterized its short-term temporal evolution.

The obtained results are consistent with previous studies in which the combined use of UAV photogrammetry and terrestrial laser scanning has been considered an effective approach for improving the completeness of the spatial representation of mining structures. In particular, the integration of UAV and TLS data has previously been applied to the three-dimensional mapping and monitoring of open-pit mining operations [15], the integration of terrestrial and aerial point clouds in mining environments [25], and the monitoring of landslide processes [28,29]. Unlike studies focused primarily on integrating spatial datasets acquired during a single survey or several closely spaced surveys, the present study emphasizes the retrospective reconstruction of successive stages of a single deformation event. For this purpose, multi-year aerial survey data and mine surveying observations were used to reconstruct the overall sequence of geometric changes, whereas TLS was used to provide a detailed characterization of the short interval of active deformation.

Each of the methods applied has its own advantages and limitations. UAV-based aerial surveying provides broad spatial coverage and enables the generation of digital surface models for multi-temporal analysis; however, its temporal informativeness is determined by survey frequency, while the comparability of the results depends on survey parameters, spatial resolution, and georeferencing quality [2,17]. TLS provides a more detailed local representation of the surface and can be applied at shorter observation intervals; however, its use is constrained by line-of-sight conditions, possible occlusion of individual areas, and requirements for the quality of spatial point cloud alignment [19,26]. GNSS and total station observations provide high-accuracy positional data for individual control points [9,11], whereas ground-based radar systems can be used for the high-frequency monitoring of rock masses [1]. Therefore, the selection of a specific method should be determined by the required spatial and temporal resolution of the observations. The combined use of

multi-temporal aerial surveys, mine surveying measurements, and TLS is particularly useful for applications requiring the spatial localization of changes, reconstruction of their long-term development, and detailed investigation of the active stage of deformation.

The practical significance of the proposed approach lies in its potential application to geotechnical monitoring programs for waste rock dumps at active mining operations. Reconstructing the sequence of deformation development, identifying its characteristic morphological features, and quantitatively assessing displacements provide a sound basis for timely engineering decisions to improve the safety of mining operations. Furthermore, the results indicate that areas exhibiting pronounced geometric changes identified from aerial survey data should be regarded as priority targets for subsequent instrument-based monitoring using methods with high temporal resolution, including terrestrial laser scanning. Overall, this study demonstrates that integrating multi-temporal aerial survey data with high-frequency terrestrial laser scanning not only enables the identification of deformation zones, but also supports the reconstruction of their development, the assessment of displacement intensity during the active stage of deformation, and a more reliable engineering interpretation of the geotechnical condition of the waste rock dump.

4.3. Applicability and Limitations of the Proposed Approach

The proposed approach can be applied to reconstruct the development of deformation in waste rock dumps and other mining structures where changes in their condition are manifested as measurable changes in surface geometry, and multi-temporal mine surveying, photogrammetric, and terrestrial laser scanning data are available. Its main advantage lies in the combined use of data with different temporal resolutions: long-term datasets enable the identification and localization of long-term geometric changes, whereas high-frequency observations provide a detailed assessment of the active stage of deformation.

For regular monitoring programs, it is preferable to maintain comparable survey parameters, including UAV and camera type, flight altitude, forward and side image overlap, and GSD, thereby reducing the influence of data heterogeneity on the detection of small-scale surface changes.

A further limitation of the present study is the absence of continuous quantitative mapping of surface changes using a DSM of difference, cloud-to-cloud comparison, or multiscale model to model cloud comparison methods. Such methods are appropriate for the detailed analysis of individual pairs of comparable digital models; however, the time series used in this study included different types of data, including profile-based mine surveying measurements, for which the direct application of continuous surface comparison methods is not possible. Therefore, in reconstructing the successive stages of deformation, priority was given to the analysis of multi-temporal cross-sections, which ensured comparability of the results obtained using different observation methods. Further development of the proposed approach may include additional spatial mapping of changes for individual pairs of photogrammetric models and point clouds.

However, the sequence of events established for the southern waste rock dump—changes in the geometry of the lower dump lift, subsequent material deposition, an increase in the height of the upper dump lift, and the subsequent development of deformation—is specific to the investigated site and should not be regarded as a universal mechanism. At other waste rock dumps, deformation development may be controlled by factors such as precipitation infiltration, changes in hydrogeological conditions, the physical and mechanical properties of the rock material, waste rock dump construction practices, or seismic effects. Therefore, the generalizable outcome of this study is the methodological framework for the spatio-temporal reconstruction of deformation, whereas interpretation of the causes of deformation development should account for the site-specific conditions.

5. Conclusions

The present study enabled the reconstruction of the successive stages of change in the southern waste rock dump of the Western Open Pit of the Zhairem Mining and Concentrating Complex. It was established that the deformation of the upper dump lift in March 2022 was preceded by changes in the geometry of the lower dump lift, restoration of the previously disturbed area through renewed material deposition, and a subsequent increase in the height of the upper dump lift. This temporal sequence allows these changes to be considered as possible factors contributing to deformation development; however, their causal influence cannot be established without additional geotechnical data.

Quantitative analysis showed a 63.19 m change in the position of the lower dump lift front, an increase in the height of the upper dump lift of approximately 17 m, and a 12.07 m decrease in surface elevation within the zone of subsequent deformation. During the first TLS observation interval, horizontal surface-profile offsets ranged from 183 to 242 mm, with an additional vertical component of +105 mm recorded at the +407 m level. During the second interval, the detected changes decreased to 24–32 mm and were below the adopted change detection threshold of approximately 42 mm; therefore, they were not interpreted as metrically reliable evidence of continued movement.

The practical significance of the proposed approach lies in establishing an integrated framework for monitoring waste rock dumps, in which multi-temporal aerial survey data are used to identify and spatially delineate zones of geometric change, mine surveying measurements are employed to analyze multi-temporal cross-sections, and terrestrial laser scanning provides a detailed quantitative assessment of active displacements. The complementary use of these methods improves the reliability of the engineering interpretation of deformation processes and can support the implementation of geotechnical monitoring programs for anthropogenic rock masses at active mining operations.

Author Contributions: Conceptualization, D.S.O. and V.V.K.; methodology, D.S.O. and V.V.K.; software, R.K.B., D.S.O. and U.A.K.; validation, D.S.O. and V.F.Y.; formal analysis, V.V.K. and U.A.K.; investigation, D.S.O., V.V.K. and V.F.Y.; resources, D.S.O. and R.K.B.; data curation, D.S.O., V.V.K. and V.F.Y.; writing—original draft preparation, V.V.K. and V.F.Y.; writing—review and editing, D.S.O., V.V.K., V.F.Y. and U.A.K.; visualization, V.V.K., V.F.Y. and R.K.B. All authors have read and agreed to the published version of the manuscript.

Funding: The study was performed within the frameworks of agreement on grant financing for young scientists in scientific and scientific-technical projects of the Republic of Kazakhstan, N 113/KMU-5-24-26, 26 June 2024, project N AR22788508.

Data Availability Statement: The data were obtained through research conducted under grant funding and are not publicly available.

Acknowledgments: The initial version of the manuscript was prepared by the authors in Russian. The translation of the article into English and its linguistic editing were performed by a professional translator.

Conflicts of Interest: The authors declare no conflicts of interest.

Abbreviations

GNSS	Global Navigation Satellite System
RTK	Real-Time Kinematic
PPK	Post-Processed Kinematic
PPP	Precise Point Positioning
CORS	Continuously Operating Reference Station
UAV	Unmanned Aerial Vehicles

TLS	Terrestrial Laser Scanning
GCP	Ground Control Points
RMSE	Root-Mean-Square Error
GSD	Ground Sampling Distance
DSMs	Digital Surface Models

References

1. Le Roux, R.; Sepehri, M.; Khaksar, S.; Murray, I. Slope Stability Monitoring Methods and Technologies for Open-Pit Mining: A Systematic Review. *Mining* **2025**, *5*, 32. [CrossRef]
2. Tsachouridis, S.; Pavloudakis, F.; Sachpazis, C.; Tsioukas, V. Monitoring Slope Stability: A Comprehensive Review of UAV Applications in Open-Pit Mining. *Land* **2025**, *14*, 1193. [CrossRef]
3. Yartseva, V.; Kazantseva, V.; Ozhigin, D.; Dolgonosov, V. The use of various types of UAVs for building digital models of a quarry and adjacent rock mass. *Sustain. Dev. Mt. Territ.* **2026**, *18*, 251–261. [CrossRef]
4. Wróblewska, M.; Kowalska, M.; Łupieżowiec, M. Slope stability analysis of post-mining dumps with the use of photogrammetric geometry measurements—A case study. *Arch. Civ. Eng.* **2023**, *69*, 171–185. [CrossRef]
5. Chand, K.; Koner, R. Large dump critical zone of interest identification and slope failure prediction using realistic 3D numerical modelling. *Geomat. Nat. Hazards Risk* **2024**, *15*, 2361809. [CrossRef]
6. Kusainova, A.; Hannanov, R.; Kaigorodova, Y.; Sitnikova, E.; Mikhnev, A.; Oleinikova, E.; Mezentseva, O. Monitoring the Stability of a Hydraulic Structure in Central Kazakhstan during a Period of Intense Precipitation in the Warm Season. *Sustain. Mar. Struct.* **2026**, *8*, 143–161. [CrossRef]
7. Bessimbayeva, O.G.; Khmyrova, E.N.; Oleinikova, E.A.; Kasymzhanova, A.E. Simulation of ash dump embankment stability. *Min. Sci. Technol.* **2023**, *8*, 303–312. [CrossRef]
8. Kosarev, N.S.; Kolesnikov, A.A.; Reznik, A.V.; Nemova, N.A.; Ozhigin, D.S. The Use of Geospatial Data in the Industrially Disturbed Land Evaluation. *J. Min. Sci.* **2023**, *59*, 1058–1065. [CrossRef]
9. Labant, S.; Bindzarova Gergelova, M.; Kuzevicova, Z.; Kuzevic, S.; Fedorko, G.; Molnar, V. Utilization of Geodetic Methods Results in Small Open-Pit Mine Conditions: A Case Study from Slovakia. *Minerals* **2020**, *10*, 489. [CrossRef]
10. Nguyen, H.V.; Pham, K.C.; Nguyen, D.B.; Nguyen, L.Q. Application of the GNSS Method in the Monitoring of Mine Surface Displacement: A Systemic Review. *Inżynieria Miner.* **2024**, *2*, 247–255. [CrossRef]
11. Pham, K.C.; Nguyen, H.V. Real-time deformation monitoring of open-pit mine dump sites using self-developed GNSS receivers: A case study of the Dong Cao Son dump site, Vietnam. *Min. Miner. Depos.* **2025**, *19*, 120–131. [CrossRef]
12. Tangadzani, J.P.; Paradzayi, C.; Muromo, T.G. Application of UAV-based photogrammetry in monitoring slope deformations in open pit mining environments: A systematic review. In Proceedings of the FIG Working Week 2024, Accra, Ghana, 19–24 May 2024. Available online: https://www.fig.net/resources/monthly_articles/2024/September_2024/12400.pdf (accessed on 10 July 2026).
13. Yartseva, V.; Ozhigin, D.; Ozhigina, S.; Ozhigin, S.; Kazantseva, V.; Dolgonosov, V. Monitoring of open pit conditions with unmanned aircraft system. In Proceedings of the 2024 IEEE 6th International Symposium on Logistics and Industrial Informatics (LINDI), Karaganda, Kazakhstan, 23–25 October 2024; pp. 145–150. [CrossRef]
14. Yiğit, A.Y.; Şenol, H.İ. Surface change and stability analysis in open-pit mines using UAV photogrammetric data and geospatial analysis. *Drones* **2025**, *9*, 472. [CrossRef]
15. Tong, X.; Liu, X.; Chen, P.; Liu, S.; Luan, K.; Li, L.; Liu, S.; Liu, X.; Xie, H.; Jin, Y.; et al. Integration of UAV-based photogrammetry and terrestrial laser scanning for the three-dimensional mapping and monitoring of open-pit mine areas. *Remote Sens.* **2015**, *7*, 6635–6662. [CrossRef]
16. Cao, D.; Zhang, B.; Zhang, X.; Yin, L.; Man, X. Optimization methods on dynamic monitoring of mineral reserves for open pit mine based on UAV oblique photogrammetry. *Measurement* **2023**, *207*, 112364. [CrossRef]
17. Cho, J.; Lee, J.; Lee, B. Application of UAV photogrammetry to slope-displacement measurement. *KSCE J. Civ. Eng.* **2022**, *26*, 1904–1913. [CrossRef]
18. Pasternak, G.; Pasternak, K.; Koda, E.; Ogrodnik, P. Unmanned aerial vehicle photogrammetry for monitoring the geometric changes of reclaimed landfills. *Sensors* **2024**, *24*, 7247. [CrossRef] [PubMed]
19. Bazarnik, M. Slope stability monitoring in open pit mines using 3D terrestrial laser scanning. In *Proceedings of the E3S Web of Conferences*; EDP Sciences: Les Ulis, France, 2018; Volume 66, p. 01020. [CrossRef]
20. Yartseva, V.F.; Ozhigin, D.S.; Dolgonosov, V.N.; Ozhigina, S.B.; Ozhigin, S.G. Study of rock mass structural features based on laser scanning results. *Kompleks. Ispolzovanie Miner. Syra Complex Use Miner. Resour.* **2026**, *338*, 72–80. [CrossRef]
21. Luu, T.A. A Review of the Application of Terrestrial Laser Scanning in Challenging Environments. *Inżynieria Miner.* **2024**, *2*, 79–85. [CrossRef]

22. Nizametdinov, F.K.; Baryshnikov, V.D.; Oralbay, A.O. Kentobe Pitwall Stability Estimation Using a Digital Geological-Geomechanical Model. *J. Min. Sci.* **2022**, *58*, 896–902. [CrossRef]
23. Zhou, D.; Wu, K.; Chen, R.; Li, L. GPS/terrestrial 3D laser scanner combined monitoring technology for coal mining subsidence: A case study of a coal mining area in Hebei, China. *Nat. Hazards* **2014**, *70*, 1197–1208. [CrossRef]
24. Nizametdinov, N.F.; Oralbay, A.O.; Igemberlina, M.B.; Batyrshaeva, Z.M. Modeling pitwall condition using laser and geoinformation technologies. *Gorn. Zhurnal* **2026**, *2*, 47–54. [CrossRef]
25. Fotheringham, M.; Paudyal, D.R. Combining terrestrial scanned datasets with UAV point clouds for mining operations. *ISPRS Ann. Photogramm. Remote Sens. Spat. Inf. Sci.* **2021**, *4*, 129–138. [CrossRef]
26. Shen, N.; Wang, B.; Ma, H.; Zhao, X.; Zhou, Y.; Zhang, Z.; Xu, J. A review of terrestrial laser scanning (TLS)-based technologies for deformation monitoring in engineering. *Measurement* **2023**, *223*, 113684. [CrossRef]
27. Liu, D.; Huang, M.; Tao, Z.; Hong, C.; Wu, Y.; Fan, E.; Yang, F. Optimized air-ground data fusion method for mine slope modeling. *J. Mt. Sci.* **2024**, *21*, 2130–2139. [CrossRef]
28. Zhou, J.; Jiang, N.; Li, C.; Li, H. A landslide monitoring method using data from unmanned aerial vehicle and terrestrial laser scanning with insufficient and inaccurate ground control points. *J. Rock Mech. Geotech. Eng.* **2024**, *16*, 4125–4140. [CrossRef]
29. Sestras, P.; Badea, G.; Badea, A.C.; Salagean, T.; Oniga, V.-E.; Rosca, S.; Bilasco, S.; Bruma, S.; Spalevic, V.; Kader, S.; et al. A novel method for landslide deformation monitoring by fusing UAV photogrammetry and LiDAR data based on each sensor's mapping advantage in regards to terrain feature. *Eng. Geol.* **2025**, *346*, 107890. [CrossRef]
30. Falabella, F.; Pepe, A.; Ostir, K.; Gubaidullina, R.; Kozmus Trajkovski, K.; Grigillo, D.; Grabrovec, V.; Hamza, V.; Pavlovcic Preseren, P.; Blaha, H.; et al. Utilization of multi-sensor remote sensing technologies for open pit mine monitoring. *Int. J. Appl. Earth Obs. Geoinf.* **2025**, *143*, 104834. [CrossRef]
31. Teng, J.; Shi, Y.; Wang, H.; Wu, J. Review on the Research and Applications of TLS in Ground Surface and Constructions Deformation Monitoring. *Sensors* **2022**, *22*, 9179. [CrossRef] [PubMed]
32. Vishnevskaya, N.A.; Ozhigina, S.B.; Ozhigin, S.G.; Kubaidullina, U.A.; Baigali, R.K.; Babazhanov, R.T. Analytical Review of the Methods of Studying Open Pit Slope Stability Under the Conditions of Mining Operations Digitalization. *Kompleks. Ispolzovanie Miner. Syra Complex Use Miner. Resour.* **2028**, *344*, 99–108. [CrossRef]
33. Balpanova, M.; Sapinov, G.; Rymkulova, A.; Ospanov, A.; Imanbayeva, S.; Tyan, S. Research on the stability of mine workings and the risk of rock caving at the Zhaysan deposit, Kazakhstan. *Min. Miner. Depos.* **2025**, *19*, 106–119. [CrossRef]
34. Matayev, A.; Zeitinova, S.; Mussin, R.; Doni, D.; Shaike, N.; Kuttybayev, A.; Iskakov, R. Research into mechanical properties of ore and rocks in the ore deposits with assessment of the mass stress state natural field. *Min. Miner. Depos.* **2024**, *18*, 71–82. [CrossRef]
35. Nizametdinov, F.; Nizametdinov, R.; Akhmatnurov, D.; Zamaliyev, N.; Mussin, R.; Ganyukov, N.; Skrzypkowski, K.; Korzeniowski, W.; Stasica, J.; Rak, Z. Geomechanical Basis for Assessing Open-Pit Slope Stability in High-Altitude Gold Mining. *Appl. Sci.* **2025**, *15*, 8372. [CrossRef]
36. Cheng, Y.; Hou, K. Open-Pit Slope Stability Analysis Integrating Empirical Models and Multi-Source Monitoring Data. *Appl. Sci.* **2025**, *15*, 9278. [CrossRef]

Disclaimer/Publisher's Note: The statements, opinions and data contained in all publications are solely those of the individual author(s) and contributor(s) and not of MDPI and/or the editor(s). MDPI and/or the editor(s) disclaim responsibility for any injury to people or property resulting from any ideas, methods, instructions or products referred to in the content.